SUPPORTING INFORMATION

An A666G mutation in transmembrane-helix 5 of the yeast multidrug transporter Pdr5 increases drug efflux by enhancing cooperativity between transport sites

Nidhi Arya, Hadiar Rahman, Andrew Rudrow, Manuel Wagner, Lutz Schmitt, Suresh V. Ambudkar, and John Golin

CONTENTS:

Results

S1. Coumarin 6 transport was not increased in the A666G mutant

The A666G mutant failed to enhance clotrimazole resistance or transport. This suggested that the A666G phenotype could be substrate-specific. Such an observation would have important bearing on mechanistic explanations for the otherwise robust enhancement of drug resistance observed in this mutant. Previous work demonstrated, however, that clotrimazole is a potent, non-competitive inhibitor of Pdr5 ATPase activity with an IC_{50} of ~ 2.0-2.5 μM when WT PM vesicles were used in the reaction *(10)*.

This inhibition might therefore impose limits on the ability of the A666G mutant to enhance transport of this substrate. We discovered, however, that coumarin 6 transport was also not enhanced by the A666G mutant.

As part of an attempt to identify additional fluorescent substrates of Pdr5 beside R6G, we tested the fluorescence quenching capability of coumarin 6. This compound that appeared to have the features of a strong Pdr5 substrate particularly because its molecular volume (267.1 cm^3 / Mol) is between two strong substrates: climbazole (248.4 cm^3 / Mol) and clotrimazole (302.0 cm^3 / Mol). It also did not inhibit Pdr5-specific ATPase activity in either WT or A666G PM vesicle preparations even at high concentrations. (Fig. S2A). When we tested the fluorescence quenching capability of the compound with WT PM vesicles, we observed that it was concentration-dependent (Fig. S2 B). The observed initial rate (IR) in a reaction containing 300nM coumarin 6 was 8.3 x 10^{-4} S^{-1}. Control experiments demonstrated that quenching was both nucleotide and Pdr5-dependent. However, when we tried to use a 500 nM concentration, there was strong, nucleotide- independent autoquenchng of coumarin 6; an observation made by others using micromolar concentrations (Li *et al.* 2005).

We compared the coumarin 6 quenching capability of PM vesicles made from WT and A666G strains (Fig. S2 C). These preparations had similar ATPase activities and representative plots are shown (n=3). In this set of plots, the observed IRs of coumarin 6 fluorescence quenching (-6.6 x 10^{-4} S^{-1} and -6.4 x 10^{-4} S^{-1}) were not significantly different once the rates were normalized to ATPase activity. The same result was also observed with two other sets of WT and A666G PM vesicle preparations (Fig.S2 D).

Coumarin 6 is not toxic to yeast cells. However, we were able to measure [^{3}H]-coumarin 6 transport in whole cells (Fig. S2 E). Transport was clearly Pdr5-dependent. The WT strain accumulated about 4x less coumarin 6 than the ΔPdr5 control. There was, however, no significant difference in the transport capability of the WT and A666G strains.

S2. Fluorescence quenching was directionally proportional to ATPase activity

We evaluated the relationship between fluorescence quenching and ATPase activities, which we measured in the Hepes buffer (pH 7.0) using the same (3 mM) concentration of ATP (Fig. S4). We did this for six preparations of A666G mutant and eight preparations of WT vesicles. The data demonstrate that although ATPase activities can vary considerably, the IRs of fluorescence quenching in the A666G mutant (blue line) were roughly 2x faster than the WT (green line) regardless of enzyme activity. Thus, a linear regression was performed and yielded slopes of -0.0092 and -0.0209 for the WT and A666G mutant respectively. This indicated that the IRs of fluorescence quenching of the A666G mutant are about 2.3x faster than the WT. The R-squared values were 0.7888 and 0.8558 respectively indicating acceptable fits.

To determine whether the slopes of the lines were different, a t-test was performed. We obtained a t-value of 0.0106 indicating a very high probability that the lines were different (0.9918).

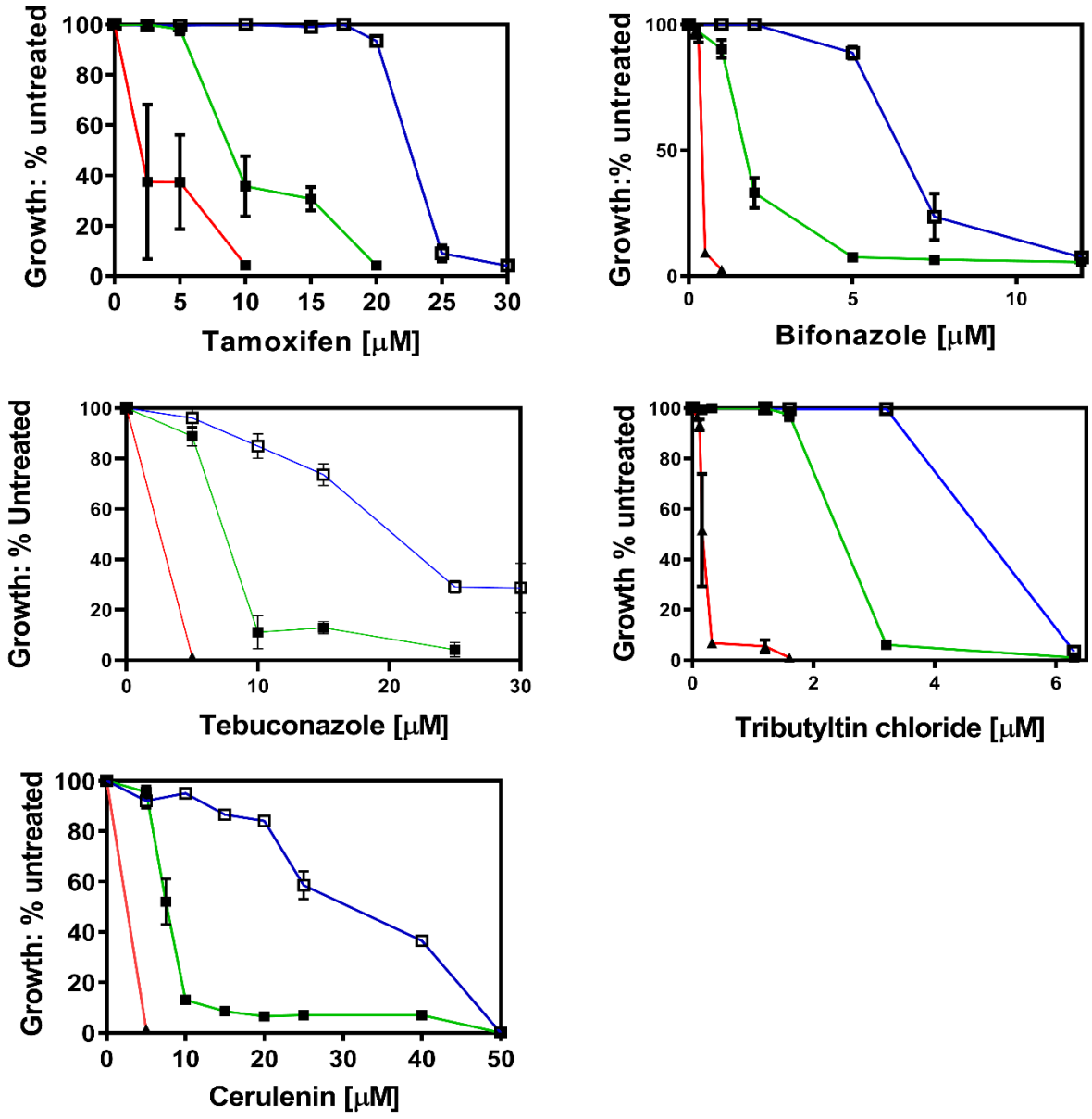

Fig. S1. The A666G mutant increases resistance to transport substrates. Cells were cultured in YPD broth at 30 °C for 48 h in the presence of drugs as described in the Experimental Procedures. YPD cultures of each strain that contained no drug served as an untreated control for growth comparisons. Cell concentration was determined at 600 nm. In this figure: ■, green WT; ▲, red, ΔPdr5; and □, blue, A666G (n = 3).

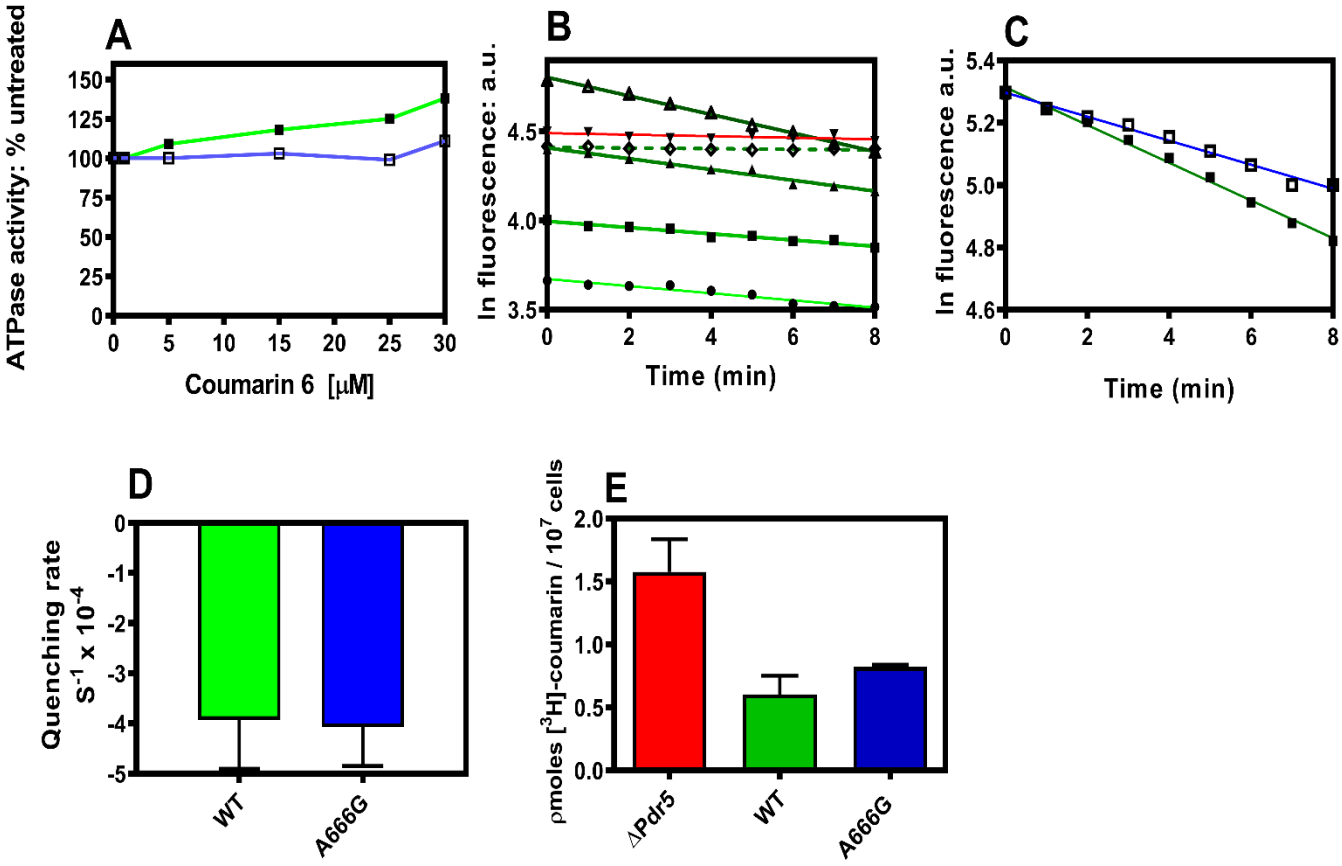

Fig. S2. Coumarin 6 transport is not enhanced by the A666G mutant. In panels (A) and (C), ■, green WT; ▲, red, ΔPdr5; and □, blue, A666G. (A) ATPase activity was monitored as described in the Experimental Procedures. Reactions were made up in Hepes transport buffer and included 16 µg purified PM vesicle protein, 3mM ATP ± coumarin 6 in a final volume of 100 µl. Incubations were performed for 8 min at 30 °C. (B) Coumarin 6 fluorescence quenching was performed as described in the Experimental Procedures. In these experiments, each sample was made up in Hepes transport buffer and contained 30 µg of purified PM vesicles, 3 mM ATP, and coumarin 6 concentrations of: ●, 100 nM; ■, 150 nM;▲, 250 nM, and Δ, 300nM. The dashed green line represents a sample in which ATP was omitted, although 250 nM coumarin 6 was present. (C) Coumarin 6 fluorescence quenching was performed with PM vesicles prepared from the WT, ΔPdr5, and A666G strains using 300 nM coumarin 6 and the same set of conditions described in panel B. Representative plots are shown (n=3). (D) The initial rates from three independent preparations of WT and A666G PM vesicles are shown. (E) [^{3}H]-coumarin 6 transport in whole cells was measured as described in the Experimental Procedures. Reactions contained 3 x 10^6 cells in a final volume of 500 µl 0.2M Hepes buffer containing 100 mM glucose and 20 µM [^{3}H]-coumarin 6. In these experiments, n =6.

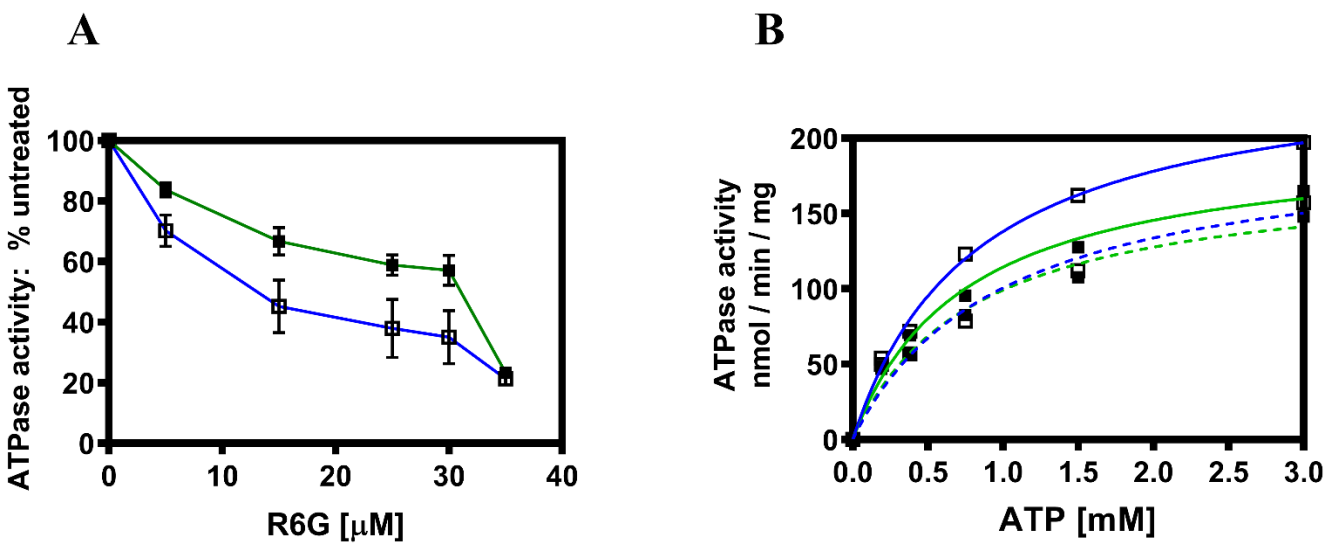

Fig. S3. The A666G mutant ATPase exhibits a modest hypersensitivity to R6G inhibition.

(A) ATPase activity was measured in Hepes (pH 7.0) buffer as described in the Experimental Procedures in the presence of R6G (0-35 μM) which was added five minutes prior to initiating hydrolysis with the addition of 3 mM ATP. In this figure: WT activity = green line, A666G activity = blue line. (B) ATPase activity was measured at various ATP concentrations in the presence of 100 nM R6G (dashed green line = WT activity; dashed blue line = A666G mutant activity). These activities were compared to corresponding reactions containing no R6G (solid green line =WT; solid blue line =A666G mutant).

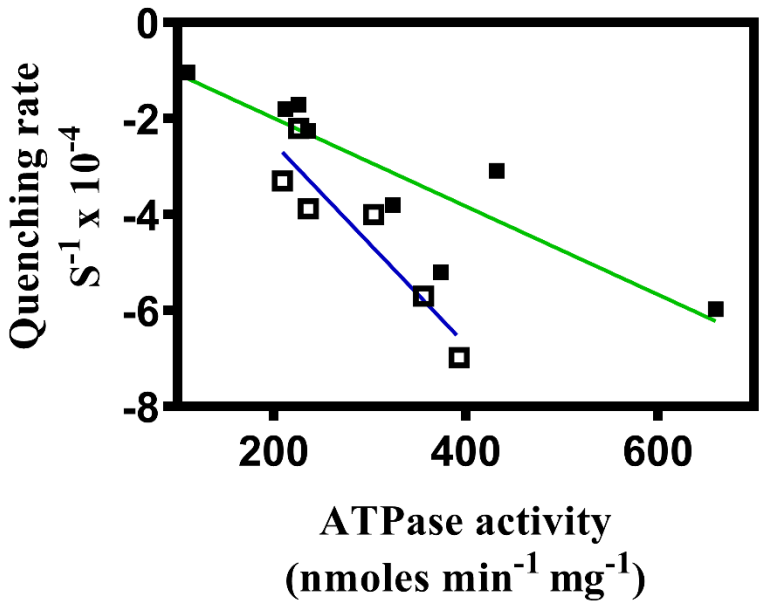

Fig. S4. The initial rates of fluorescence quenching are directly proportional to ATPase activity. Fluorescence quenching experiments were performed with independent PM preparations of the WT and A666G mutant. Initial quenching rates were determined by linear regression performed on each plot shown in panel B of fig S2. The rates were plotted versus ATPase activity determined in Hepes transport buffer with 3mM ATP using the assay described in the Experimental Procedures.

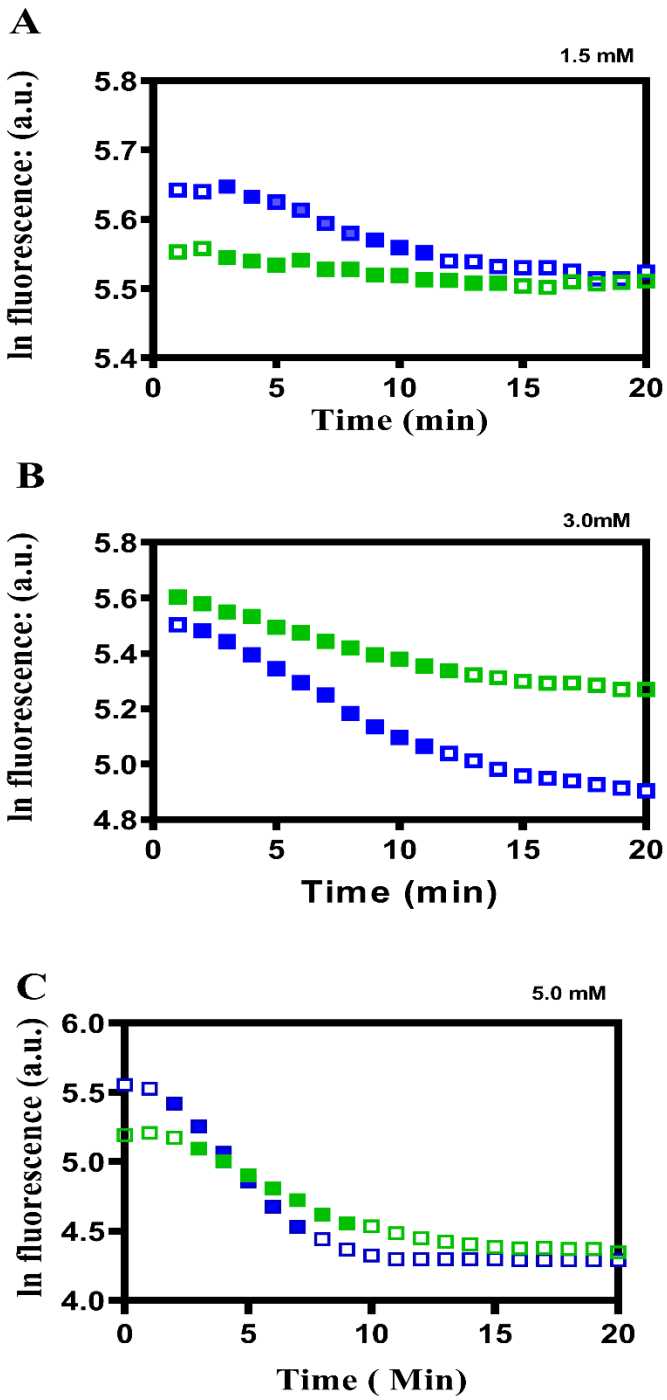

Fig. S5. Representative plots of fluorescence quenching performed with 1.5, 3.0, and 5.0 mM ATP. Fluorescence quenching experiments were performed as described in the Experimental Procedures. We plotted the ln of the fluorescence values taken at one-minute intervals. WT: green; A666G: blue. The linear portions of the curves used to determine the IRs have solid symbols.

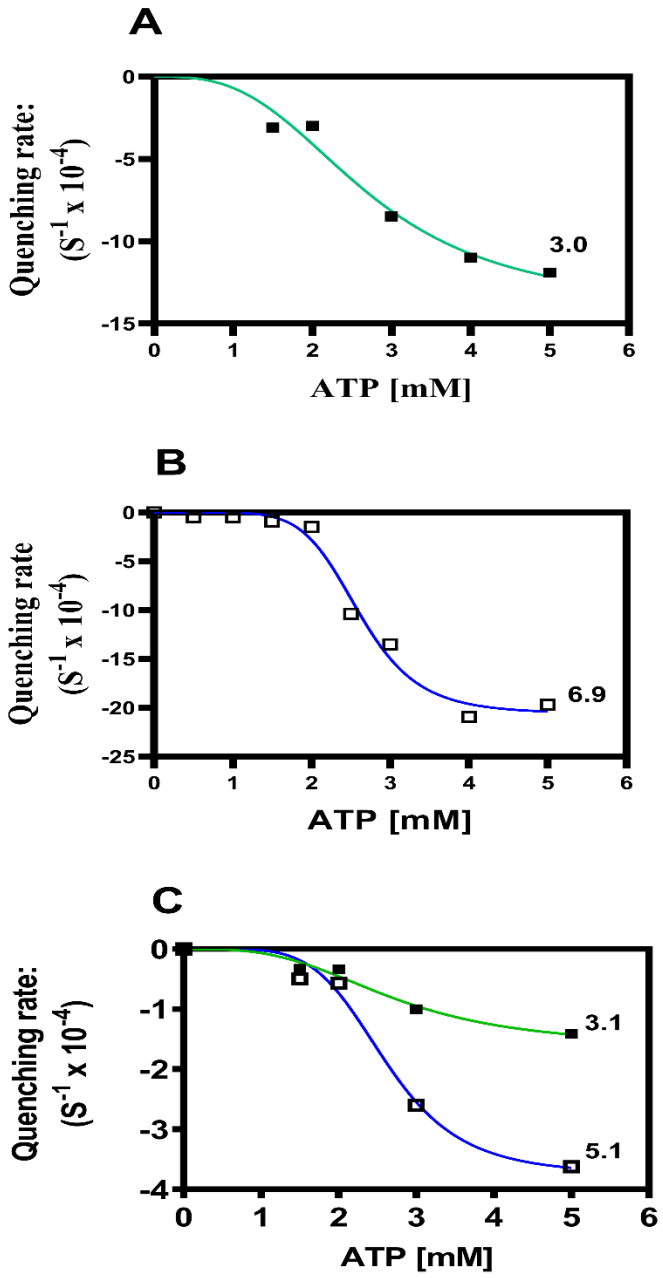

Fig. S6. The A666G mutant exhibits increased cooperativity between transport sites. The experiments shown in this figure are analogous to those illustrated in Fig. 8. The quenching reaction was performed as described in the Experimental Procedures. In addition to the data found in Fig. 8, we did the analogous experiment with (A) an additional WT and (B) A666G mutant preparations that were made and assayed independently of each other. (C) We also performed the same assay with PM vesicles that were made using the older protocol and were therefore were not as active. The number at the bottom of each curve is the Hill coefficient. In this figure: ■, green WT; and □, blue, A666G.